

Nitrogen pair-induced temperature insensitivity of the band gap of GaNSb alloys

W. M. Linhart,^{1,2, a)} M. K. Rajpalke,¹ M. Birkett,¹ D. Walker,³ M. J. Ashwin,³ and T. D. Veal^{1, b)}

¹⁾*Stephenson Institute for Renewable Energy and Department of Physics, School of Physical Sciences, University of Liverpool, Liverpool L69 7ZF, United Kingdom*

²⁾*Faculty of Fundamental Problems of Technology, Wrocław University of Science and Technology, Wybrzeże Wyspiańskiego 27, 50-370 Wrocław, Poland*

³⁾*Department of Physics, University of Warwick, Coventry CV4 7AL, United Kingdom*

The temperature dependence of the band gap of GaN_xSb_{1-x} films with $x \leq 1.3\%$ has been studied in the 1.1–3.3 μm (0.35–1.1 eV) range using infrared absorption spectroscopy between 4.2 and 300K. As with other dilute nitride semiconductors, the temperature dependence of the band gap is reduced by alloying with nitrogen when compared to the host binary compound. However, for GaNSb, the smallest variation of the band gap with temperature is observed for samples with the lowest N content for which the band gap is almost totally insensitive to temperature changes. This contrasts with the more widely studied GaN_xAs_{1-x} alloys in which the band gap variation with temperature decreases with increasing N content. The temperature-dependent absorption spectra are simulated within the so-called band anticrossing model of the interaction between the extended conduction band states of the GaSb and the localized states associated with the N atoms. The N next-nearest neighbor pair states are found to be responsible for the temperature insensitivity of the band gap of the GaNSb alloys as a result of their proximity to the conduction band edge giving them a more pronounced role than in GaNAs alloys.

The temperature dependence of the fundamental band gap energy of semiconductors represents a basic material-specific property which is of considerable practical and also theoretical interest. It is known from many experimental results that the band gap of a semiconductor decreases monotonically with increasing temperature. The two main contributions to this are shifts of the band edges due to: (i) dilation of the lattice constant with increasing temperature; and (ii) the temperature dependent electron-phonon interaction.¹ There are several commonly employed models or parameterizations of the temperature dependence of the band gap of semiconductors. These include the Bose-Einstein^{2,3} and O'Donnell models.⁴ However, the most frequently used formula for approximate parameterization of band gap energy as a function of temperature is the one proposed by Varshni, $E_g(T) = E_g(0) - AT^2/(B + T)$ where A and B are constants.¹

The temperature dependence of the band gap of conventional III-V semiconductors such as GaAs, GaSb or InP can be modified by the substitution of nitrogen onto the group V sub-lattice. It has been shown that the incorporation of a few percentage of nitrogen in Ga(In)As reduces the temperature-induced shift of the band gap energy by 12% in GaInNAs⁵ and 40% in GaNAs⁶ compared to GaAs. The effect has been ascribed to the interaction of temperature-insensitive localized N states with extended band states that have a temperature dependence close to that of GaAs^{6,7}. For GaNAs, the temperature dependence of the band gap decreases as the N content is increased, suggesting the possibility of increased

temperature insensitivity of the band gap, a desirable material property for device applications.

Introducing a small amount of nitrogen into the host III-V semiconductor causes a strong reduction of the band gap energy. This reduction has been already observed in the dilute nitrides GaNAs⁶, GaInNAs⁵, GaNP⁹, GaNSb⁸ and also in InNAs¹⁰ and explained by a two level conduction band anticrossing model (BAC) where the interaction between the host conduction band and resonant nitrogen level results in the formation of two nonparabolic subbands^{11,12}. Recent studies of GaNSb have shown that a three level BAC model, where additional N next-nearest-neighbor pair states play a significant role,^{13,14} much better reproduces the evolution with N content of the lowest absorption edge¹⁵. Additionally the linear combination of isolated nitrogen states (LCINS) model proposed by O'Reilly *et al.* has also given good results.^{16,17}

Unlike in most other cases, where a reduction in band gap energy is achieved by inserting an element that increases the lattice constant, nitrogen accomplishes this and at the same time reduces the lattice constant. These phenomena have important implications for developing new materials systems. For example, by substituting specific ratios of nitrogen and indium into GaAs, forming GaInNAs, the lattice parameter can be matched to that of GaAs while simultaneously reducing the band gap¹⁸. This approach also offers the prospect of lattice matched GaInNSb and GaNSbBi alloys with tunable band gaps for mid-infrared optoelectronic devices, including sources and detectors for the 2-5 micron atmospheric transmission window, thermophotovoltaics and lasers.^{15,19} For these applications, a temperature independent band gap is a desirable property, but there are no previous reports of the GaNSb band gap as a function of temperature.

^{a)}Electronic mail: wojciech.linhart@gmail.com

^{b)}Electronic mail: T.Veal@liverpool.ac.uk

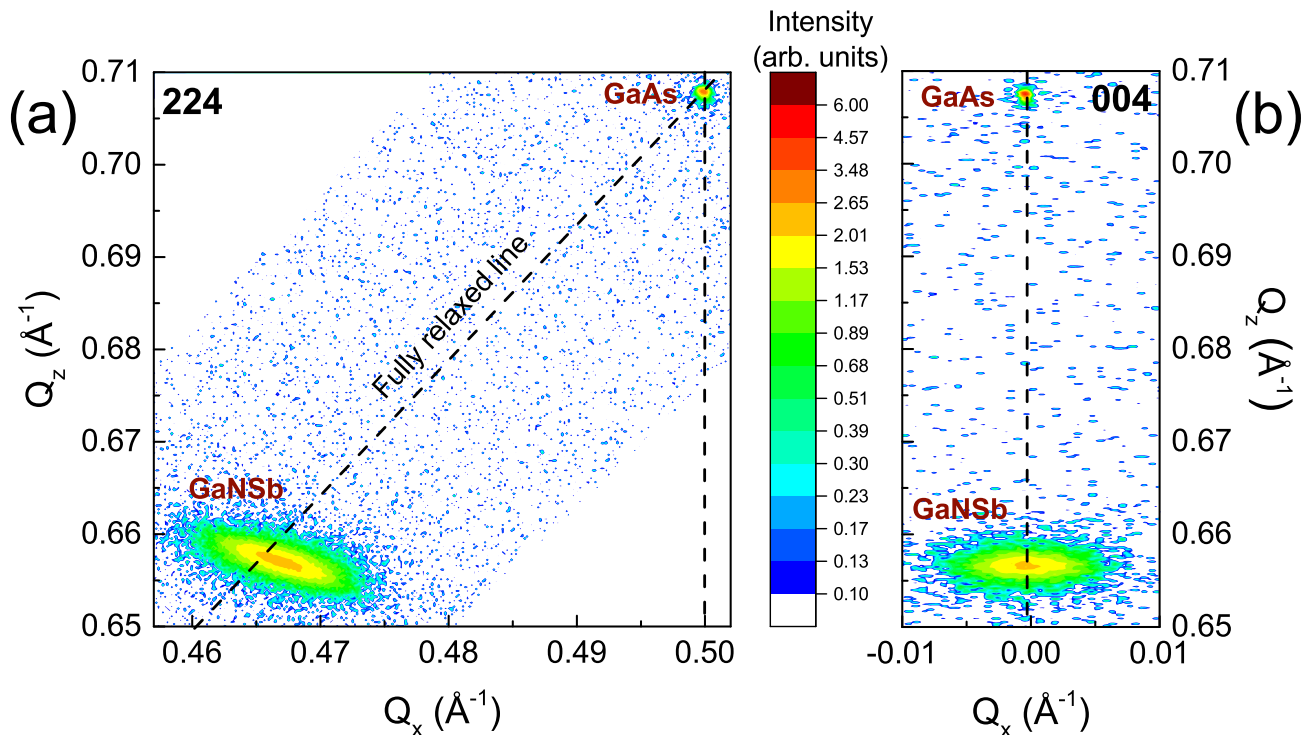


FIG. 1. X-ray diffraction reciprocal space maps from a $2\ \mu\text{m}$ -thick GaNSb film grown on a GaAs(001) substrate for (a) the 224 and (b) the 004 reflections. These RSMs indicate that $1.30\pm 0.05\%$ of the anion sublattice sites contain N atoms and that the film is $95.5\pm 0.5\%$ relaxed.

Here, unexpected temperature insensitivity of the band gap of GaNSb alloys is demonstrated with least temperature dependence for the lowest N content. (The models employed here based on perturbation theory approaches do not have a threshold at which the BAC behaviour switches off, but there will be some threshold below which the models no longer apply. Here we have not explored samples with an N content below 0.18% of the anion sublattice. However, previous tight binding results for GaNSb depict the band anticrossing phenomenon for 3 N atoms out of 864 anion lattice sites, a N content of 0.35% (Ref. 20) and magneto tunnelling spectroscopy has previously given experimental evidence of the band anticrossing E versus k dispersion for GaNAs with a little as 0.08% N (Ref. 21). First principles calculations of GaNAs and GaNSb are consistent with these experimental and tight binding results.²²) This temperature insensitivity is found to be due to the presence of a localized state associated with N pairs below the conduction band edge of the host GaSb material. This behavior is explained within the three level BAC model. Such a strong degree of temperature insensitivity has not been observed before in the more widely studied Ga(In)NAs alloys, where the N pair states in this material do not play such a significant role and the simple two level BAC model is sufficient to describe the changes of the band gap as a function of temperature.⁶

The samples used in this work are $2\ \mu\text{m}$ thick $\text{GaN}_x\text{Sb}_{1-x}$ films grown by plasma assisted molecular beam epitaxy (MBE) on semi-insulating GaAs(001) substrates at QinetiQ Ltd., Malvern. The N contents determined from high-resolution x-ray diffraction reciprocal space mapping measured on a Panalytical XPert Pro MRD equipped with a 4-bounce Ge 220 Hybrid Monochromator giving pure $\text{Cu K}\alpha_1$ radiation and a triple-axis monochromator. The N content was varied by changing the substrate temperature with a fixed growth rate of $0.8\ \mu\text{m h}^{-1}$ (Ref. 23). A GaSb reference film of $2\ \mu\text{m}$ thickness was grown by MBE on semi-insulating GaAs(001) at the University of Warwick. Reflectance and transmittance measurements were performed in the temperature range from 4 to 300K using a Bruker Vertex 70V Fourier-transform infrared spectrometer (FTIR), using a liquid nitrogen-cooled HgCdTe detector with a working range between 0.05 and 1.2 eV and using a continuous flow helium cryostat (Oxford Optistat CF-V). The absorption coefficient, α , was calculated from the transmission and reflectance data using equation (1) in Ref. 15. A gold mirror was used as the reflection standard. The angle of incidence for reflection and transmission measurements was 11° with respect to the surface normal of the sample. The FTIR spectra were recorded with the resolution set to 1 meV. Hall effect measurements using the Van der Pauw configuration were used

to determine the carrier concentration and mobility at room temperature (295 K) and liquid nitrogen temperature (77 K).

The reciprocal space maps (RSMs) for the 224 and 004 reflections for one of the samples are shown in Fig. 1 in reciprocal lattice units. X-ray diffraction RSMs of the $\text{GaN}_x\text{Sb}_{1-x}$ samples grown on GaAs substrates were used to determine the alloy composition. As the $\text{GaN}_x\text{Sb}_{1-x}$ epilayers are $\sim 2 \mu\text{m}$ -thick they are expected to be close to 100% relaxed. In order to be able to account for any tetragonal distortion, two dimensional reciprocal space mapping of the 224 and 004 Bragg peaks has been performed to enable the composition and degree of relaxation to be determined. The data in Fig. 1 is from a film determined to have a N content of 1.3% and relaxation of 95.5%. This degree of relaxation can be seen in the 224 RSM where the GaNSb epilayer peak is close to the line corresponding to full relaxation. The N content of the films was found from the RSMs to be in the range of 0.18 to 1.3% of the group V sublattice with 95–98% relaxation.

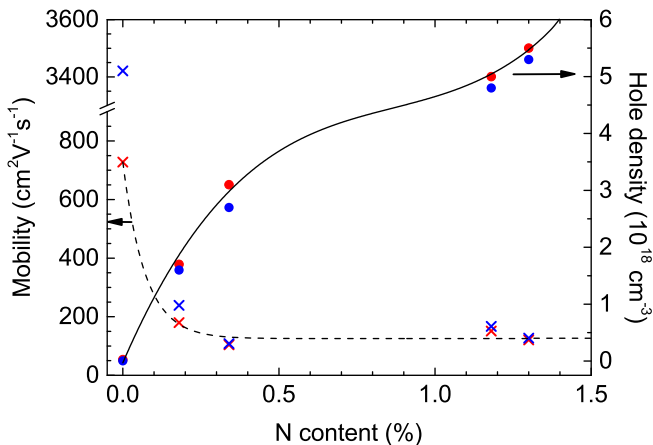


FIG. 2. Hole concentration (circles) and carrier mobility (crosses) as a function of N content recorded at 77 K (blue) and room temperature (red). The room temperature data has been reported previously in Ref. 24. The lines are guides to the eye.

Hall effect results are shown in Fig. 2 for 77 and 295 K. All the films are *p*-type with hole density (mobility) in the range $(1.6\text{--}5.5) \times 10^{18} \text{ cm}^{-3}$ ($180\text{--}104 \text{ cm}^2\text{V}^{-1}\text{s}^{-1}$) for all the $\text{GaN}_x\text{Sb}_{1-x}$ films and $2 \times 10^{16} \text{ cm}^{-3}$ ($730 \text{ cm}^2\text{V}^{-1}\text{s}^{-1}$) for the GaSb film.

The absorption spectra obtained at different temperatures for the *p*-type GaSb layer grown on a GaAs substrate are shown in Fig. 3(a). The exciton peak appears up to 90 K. The band gap behavior as a function of temperature is shown in Fig. 4(a); values from 100 to 300 K were found using standard linear extrapolation to the background intensity of α^2 versus $h\nu$ curves, while values from 4.2 up to 90 K were obtained using the exciton peak position plus the Rydberg energy of 1.4 meV.²⁵ The oscillations below the absorption onset for each temper-

ature are due to the Fabry-Perot interference associated with the GaSb film thickness. The band gap decreases by 92 meV between 4 and 300 K.

Absorption spectra for different temperatures of two $\text{GaN}_x\text{Sb}_{1-x}$ films are shown in Fig. 3(b) and (c). In each sample, the absorption coefficient generally increases with increasing temperature, which is typical for direct band-gap semiconductors. With increasing temperature the absorption edges shift to lower energies, while the line shape (base line and slope) remains essentially unchanged. However, the shift of the lowest absorption edge with temperature is much smaller than the shift of absorption edge of the host GaSb and becomes greater for the samples with higher N content; the absorption edge shifts to lower energy between 4 and 300K are 40, 74 and 84 meV for 0.18, 0.34 and 1.3% N, respectively. This behavior is opposite to the case of GaNAs, where the absorption edge shift is reduced with increasing N content^{6,7}.

The effect observed here for GaNSb can be described by the three level BAC model. The band structure of $\text{GaN}_x\text{Sb}_{1-x}$ with $x = 0.013$ is shown in Fig. 3(d) and has been calculated using a three level BAC model with impurity levels associated with isolated N atoms and N second-nearest-neighbor pairs, where a Ga atom has two N neighbors, interacting with the host conduction band, resulting in the formation of three nonparabolic subbands,^{14,15,17} described by the Hamiltonian

$$H = \begin{bmatrix} E_C(k) & V_{MN} & V_{MNN} \\ V_{MN} & E_N & 0 \\ V_{MNN} & 0 & E_{NN} \end{bmatrix}, \quad (1)$$

where E_N and E_{NN} are the isolated N and N pair impurity level energies, and $V_{MN} = \beta_N x_N^{1/2}$ and $V_{MNN} = \beta_{NN} x_{NN}^{1/2}$ denote the BAC coupling matrix elements. Here the statistically expected concentration of N pairs, x_{NN} , is $6x^2$, where x is the total N content, and the concentration of isolated N atoms, x_N , is taken as $x - 2x_{NN}$. Additionally, it should be noted that the host GaSb conduction band, $E_M(k)$, includes the Kane nonparabolicity, due to interactions with the light-hole, heavy-hole and split-off bands, described by the (4×4) $\mathbf{k} \cdot \mathbf{p}$ Hamiltonian introduced by Pidgeon and Brown in Ref. 26. The anti-crossing between the host conduction band, N level and N pair level is clear, creating three subbands (E_1 , E_2 and E_3 - see Fig. 3 (d)). The lower of these two subbands, of largely conduction band *s*-like character close to Γ , is below the conduction band minimum of the host semiconductor (GaSb), causing a reduction of the fundamental band gap. With increasing N content, the anticrossing interaction becomes stronger, leading to a reduction in energy of the E_1 and E_2 bands and an increase in the energy of the E_3 band, increasing their separation and reducing the fundamental band gap.

The BAC parameters used in the modelling were optimized to reproduce the experimentally determined evolution with temperature and N content of the band

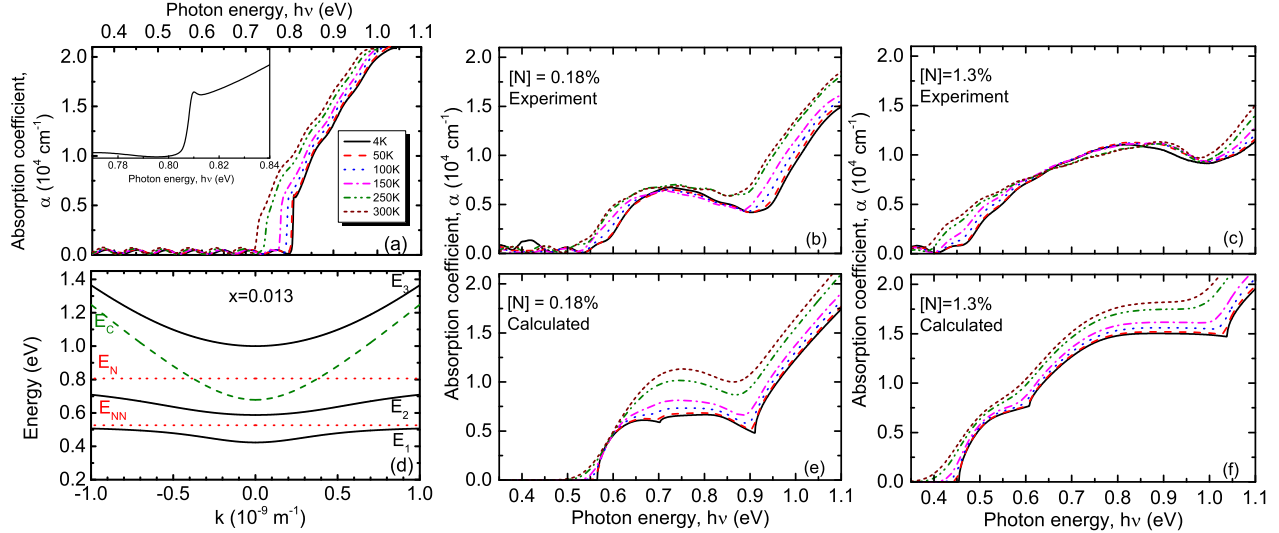


FIG. 3. (a) Absorption spectra taken at different temperatures of GaSb grown on GaAs. The inset shows the excitonic absorption peak of the 4 K data over a narrow energy range. (b) and (c) Absorption spectra of $\text{GaN}_x\text{Sb}_{1-x}$, with $x = 0.0018$ and 0.013 respectively. (d) Band structure close to the Γ point of the Brillouin zone for $\text{GaN}_x\text{Sb}_{1-x}$ with $x=0.013$, calculated using three level BAC model. The dashed line denotes the host (GaSb) conduction band, the solid lines demonstrates the subbands and the dotted lines demonstrate the positions of N impurities levels. (e) and (f) Calculated absorption spectra of $\text{GaN}_x\text{Sb}_{1-x}$, with $x = 0.0018$ and 0.013 respectively.

edge positions from the absorption onsets. Previously we reported, from three level BAC modelling of room temperature absorption data, the impurity levels to be $E_N = 0.82$ eV and $E_{NN} = 0.48$ eV above the valence band maximum¹⁵. Here, the measurements were performed over a wide temperature range and the modelling additionally includes band gap renormalization and broadening, enabling the impurity level values to be determined more accurately, giving values of $E_N = 0.85$ eV and $E_{NN} = 0.55$ eV above the valence band maximum. By fitting to the absorption onsets values, the optimum values of β_N and β_{NN} were found to be 2.3 eV and 3.25 eV, respectively, similar to those reported in Ref. 15.

Calculated absorption curves are shown in Fig. 3(e) and (f). The calculated absorption spectra were simulated using the method described by Perlin *et al.*²⁷, extended to include N pair states as reported in Refs 15 and 17. It is based on the calculation of the joint density of states for each electronic transition. It also includes band gap renormalization whereby interactions between the free carriers and with the ionized impurities lead to a narrowing of the band gap in semiconductors.²⁸ The calculated band gap renormalization for all the GaNSb samples is in the range 40-50 meV. Additionally, to account for extrinsic broadening and temperature dependent broadening of experimental spectra due to electron-phonon interactions, a Gaussian function was convoluted with the simulated energy-dependent absorption coefficient. The broadening parameter, $\Gamma(T)$, of the Gaussian varied with temperature according to the formula, $\Gamma(T)$

$= \Gamma(0) + \Gamma_{LO} / [\exp(\theta_{LO}/T) - 1]$, where Γ_{LO} is the electron-longitudinal optical (LO) phonon coupling constant, and θ_{LO} is the LO phonon temperature. The parameter $\Gamma(0)$ accounts for intrinsic broadening and extrinsic broadening mechanisms such as impurity and alloy scattering.²⁹

The absorption edges as a function of temperature of GaSb and $\text{GaN}_x\text{Sb}_{1-x}$ with different N compositions of 0.18%, 0.34% and 1.3% are presented as open circles with error bars in Fig. 4. The temperature dependence of the band gap energy of the GaSb was parameterized using the conventional Varshni relation, $E_g(T) = E_g(0) - AT^2/(B + T)$. $E_g(0)$ is the band gap at $T = 0$ K while A and B are the Varshni coefficients. The parameters fitted for GaSb were found to be $E_g(0) = 0.811$ eV, $A = 4.97 \times 10^{-4}$ eV/K, and $B = 185$ K which are very close to Vurgaftman *et al.*'s recommended values.³⁰ These values were used to describe the temperature dependence of the host GaSb band gap in the modelling of the temperature dependent GaNSb absorption spectra. Very similar fits to the temperature dependence of the band gap of GaSb were also obtained using the Bose-Einstein formula.²

The calculated variation of the band gap with temperature is shown for the GaNSb samples by the solid lines in Fig. 4. This shows that the three level BAC model predicts only 1.3, 2.5 and 29 meV reduction in band gap between 4 and 300 K for GaNSb with N contents of 0.18, 0.34 and 1.3%, respectively. This reduction of the band gap in this temperature range is significantly less than the corresponding measured reduction of the

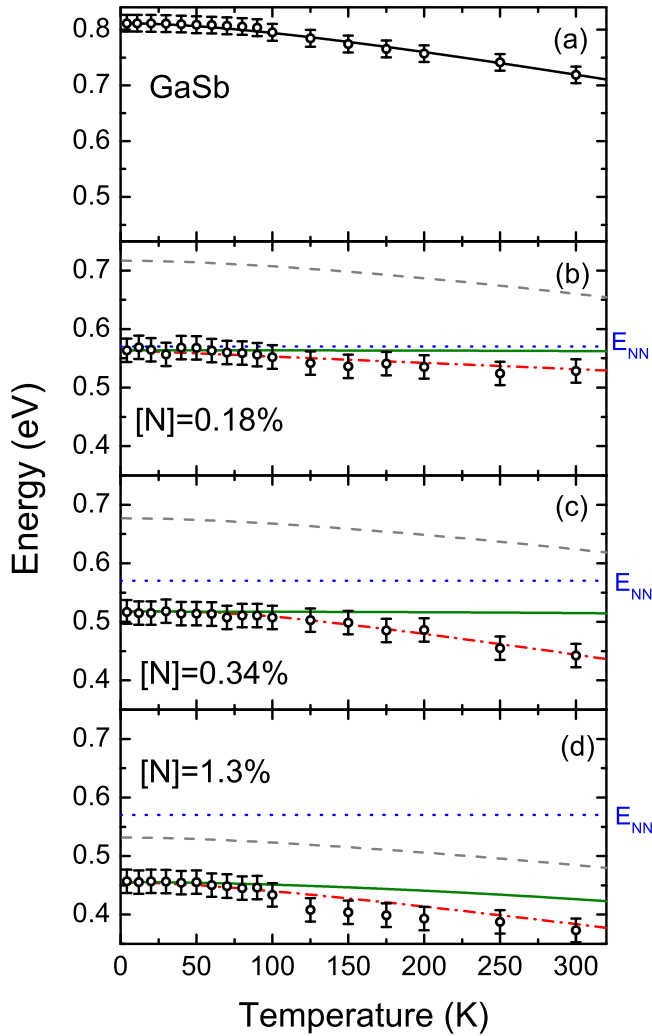


FIG. 4. The lowest energy absorption onsets (open circles with error bars) as a function of temperature for $\text{GaN}_x\text{Sb}_{1-x}$ samples with (a) $x=0$, (b) $x=0.0018$, (c) $x=0.0034$, and (d) $x=0.013$. For (a), the solid line is the result of Varshni fitting of the temperature dependence of the absorption edge of GaSb. The other solid lines depict the evolution of the lowest conduction subband, with respect to the valence band maximum, as a function of temperature modeled with the three level BAC model neglecting broadening. The dot-dashed lines show the evolution of the lowest conduction subband as a function of temperature modeled with the three level BAC model including broadening. The dashed lines show the evolution of the lowest conduction subband as a function of temperature modeled with the two level BAC model. The dotted lines represent the energy of the N pair level, used in the modelling.

absorption edges of 40, 74 and 84 meV. The addition of temperature dependent broadening to the calculated absorption spectra is required to reproduce the experimental temperature dependence of the absorption edges; the calculated variation of the absorption edge with temperature including this broadening for the different samples is depicted by the dot-dashed lines in Fig. 4. Once broad-

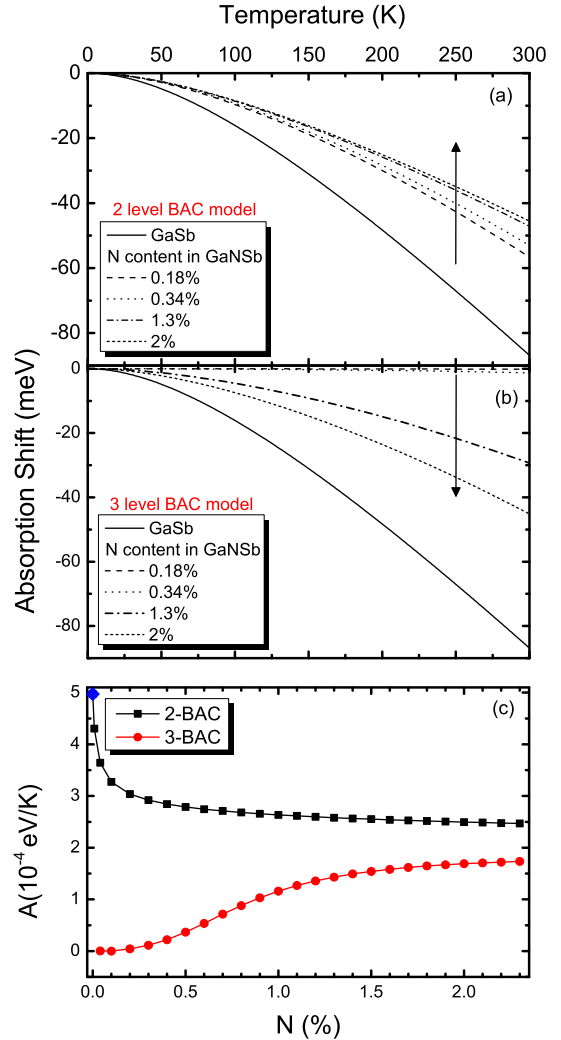


FIG. 5. Temperature-dependent energy shift of the absorption edge calculated for $\text{GaN}_x\text{Sb}_{1-x}$ using (a) two level BAC model and (b) three level BAC model. The arrows show the direction of the trend as a function of N contents. (c) Comparison of modeled Varshni A parameters as a function of composition, calculated using two level BAC (square) and three level BAC (circle). In the modelling, the parameter B was kept constant and equal to the value of GaSb 184.6 K. The diamond mark at $N=0\%$ corresponds to the A value of GaSb.

ened, the absorption edge onset energy of each calculated absorption spectrum is taken to be the result of fitting the linear portion of α^2 versus $h\nu$ and extrapolating to zero absorption coefficient. The maximum broadening, Γ , which occurs at the highest temperature of 300 K, is in the range 50-70 meV for all the GaNSb samples. This is in the range of the broadening previously reported for GaAs, GaP and GaN.³¹

Figure 5 shows the temperature dependence of the energy shift of the band gap of $\text{GaN}_x\text{Sb}_{1-x}$ alloys calculated using two different models: the two level BAC model, neglecting the N pair level (in Fig. 5 (a)) and the three level

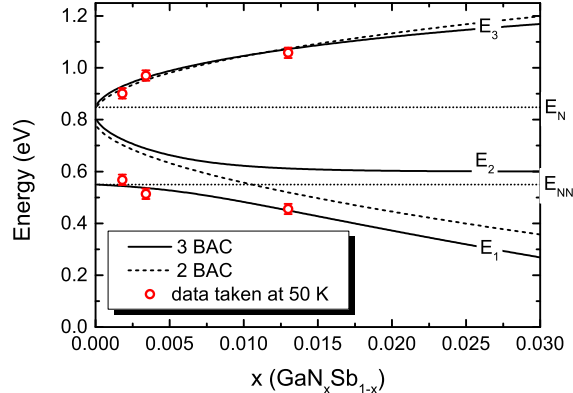


FIG. 6. The evolution of the E_1 , E_2 , and E_3 subbands as a function of N content, x , at a temperature of 50K, calculated with the two level BAC model (dotted lines) and the three level BAC model (solid lines). The isolated N level, E_N , and N pair levels, E_{NN} , are shown as dashed lines.

BAC model including the N pair level (in Fig. 5 (b)). In contrast to $\text{GaN}_x\text{As}_{1-x}$ alloys⁷, a small temperature dependence of the band gap is observed for the very lowest N content of 0.18% - 40 meV between 4 and 300K, corresponding to a band gap reduction of about 1 meV and a ~ 39 meV downward shift of the absorption edge due to electron-phonon interaction-induced broadening. This difference from GaNAs is because for that material, the N pair level does not play a significant role and so the two level BAC model is sufficient to describe the absorption edge evolution as a function of temperature.²⁰ In the case of $\text{GaN}_x\text{Sb}_{1-x}$, the N pair level has a much greater influence on the evolution of the absorption edge as a function of both N content and temperature.

For the lowest N content of 0.18%, the density of states is very small for the lowest conduction subband, therefore the absorption edge is determined by a combination of E_1 and E_2 subbands. The middle E_2 subband is repelled by the lowest E_1 subband preventing it from moving below the N pair level, even though increased temperature drives it downwards in energy. For the largest N content of 1.3%, the density of states for the lowest conduction subband E_1 is much larger; therefore it fully determines the lowest energy absorption edge. In this case, the subband which determines the lowest absorption edge is not trapped by repulsion by a nearby level so the temperature dependence is larger.

In Fig. 6, the calculated evolution of the subband energies with N content is plotted for a temperature of 50 K along with the experimental absorption onsets. This shows that the 3-level BAC model provides a better description than the 2-level BAC model for all three N contents measured here. But it is expected that for some composition below 0.18% N, the 2-level BAC model will provide the best description of absorption data.

In order to consider the effects of lifetime broadening,

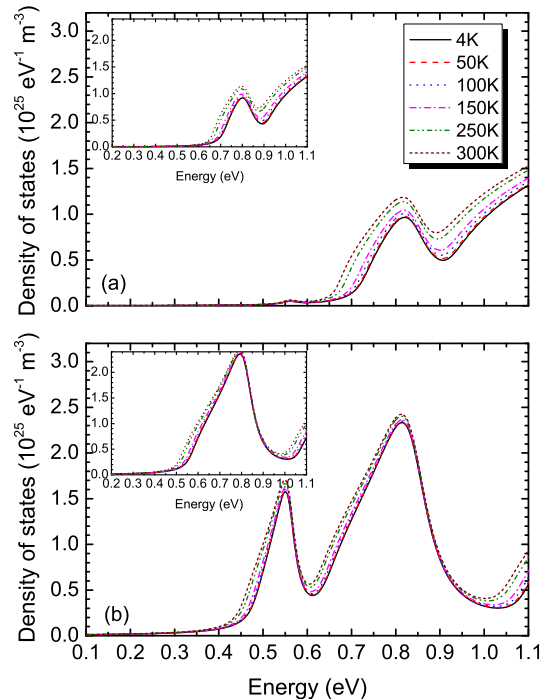


FIG. 7. Conduction band density of states for $\text{GaN}_x\text{Sb}_{1-x}$ with (a) $x=0.0018$, and (b) $x=0.013$, calculated using many impurity Anderson model including N pair states and lifetime broadening. The insets show corresponding conduction band density of states without the N pair states contribution.

the densities of states for different temperatures, calculated using Green's function implementation of the many impurity Anderson model³² for two GaNsb compositions are presented in Figure 7 and the insets contain the density of states calculated using the two level BAC model. These calculations confirm the findings detailed above from comparison of the experimental absorption spectra with those calculated using the three level BAC model. That is, the presence and energy position of the N pair level strongly influences the band gap evolution with N content and also its temperature dependence.

The change of temperature dependence of the band gap as a function of N content can be illustrated by the evolution of the derived Varshni A parameter as a function of composition. The determined Varshni parameter A as a function of composition, using two level and three level BAC models is presented in Fig. 5(c). The parameter B was kept constant and equal to the value for the host GaSb. In the two level BAC model, the parameter A monotonically decreases with increasing N content and asymptotically tends to 2.5×10^{-4} eV/K - this corresponds to greater absorption edge shift for low N content and smaller absorption edge shift for higher N contents. This is the phenomenon previously observed for GaNAs.⁷ Additionally, the slope of the curve is negative and changes from being very steep for low N content to

shallow for higher N contents, indicating that the amount of absorption edge shift with temperature plateaus with increasing N content.

For the case of three level BAC, the situation is different. Here, the parameter A monotonically increases with increasing N content from $A \sim 0$ eV/K and this corresponds to greater absorption edge shift with increasing N content. The slope of the curve is always positive, but it changes from being initially shallow (up to 0.25% N) to being steep (between 0.25 and 1.5% N) and then plateaus with increasing nitrogen concentration. Hence, the rate of change of absorption edge shift is small for very low N concentration, increases and finally reduces again with increasing N content. These phenomena are illustrated by the arrows in Fig. 5(a) and (b).

In conclusion, the temperature dependence of the optical gap of $\text{GaN}_x\text{Sb}_{1-x}$ films has been studied by FTIR absorption spectroscopy and understood in terms of a three level band anticrossing model in the range of 4–300K. The experimental data have been well reproduced using the three level BAC model modified including the effects of band gap renormalization and Gaussian broadening. By the comparison of experimental to modeled spectra, the position of isolated N and N pair levels have been determined to be $E_N = 0.85$ eV and $E_{NN} = 0.55$ eV. A decrease in the energy of the absorption onset has been observed with increasing temperature. However, an unexpected trend was found of energy gap change with temperature as a function of N content - the temperature insensitivity of the band gap is greatest for $\text{GaN}_x\text{Sb}_{1-x}$ samples with low N content in contrast to dilute $\text{GaN}_x\text{As}_{1-x}$ alloys.

The work at Liverpool and Warwick was supported by the University of Liverpool and the Engineering and Physical Sciences Research Council (EPSRC) under Grant Nos. EP/G004447/2 and EP/H021388/1. W. M. Linhart acknowledges support from the National Science Center (NCN) grant No. 2014/13/D/ST3/01947. J. D. Aldous is acknowledged for preliminary absorption measurements using liquid nitrogen for sample cooling. L. Buckle and T. Ashley are gratefully acknowledged for the MBE growth of the GaNSb films.

¹Y. P. Varshni, *Physica* **34**, 149 (1967).

²S. Logothetidis, L. Vina, and M. Cardona, *Phys. Rev. B* **31**, 947 (1985).

³P. Lantenschlager, M. Garriga, S. Logothetidis, and M. Cardona, *Phys. Rev. B* **35**, 9174 (1987).

⁴K. P. O'Donnell and X. Chen, *Appl. Phys. Lett.* **58**, 2924 (1991).

⁵P. Perlin, S. G. Subramanya, D. E. Mars, J. Kruger, N. A.

Shapiro, H. Siegle, and E. R. Weber, *Appl. Phys. Lett.* **73**, 3703 (1998).

⁶K. Uesugi, I. Suemune, T. Hasegawa, T. Akutagawa, and T. Nakamura, *Appl. Phys. Lett.* **76**, 1285 (2000).

⁷I. Suemune, K. Uesugi, and W. Walukiewicz, *Appl. Phys. Lett.* **77**, 3021 (2000).

⁸P. H. Jefferson, T. D. Veal, L. F. J. Piper, B. R. Bennet, C. F. McConville, B. N. Murdin, L. Buckle, G. W. Smith, and T. Ashley, *Appl. Phys. Lett.* **89**, 111921 (2006).

⁹J. N. Baillargeon, P. J. Pearah, K. Y. Cheng, G. E. Hofer, and K. C. Hsieh, *J. Vac. Sci. Technol. B* **10**, 829 (1992).

¹⁰T. D. Veal, L. F. J. Piper, P. H. Jefferson, I. Mahboob, C. F. McConville, M. Merrick, T. J. C. Hosea, B. N. Murdin, and M. Hopkinson, *Appl. Phys. Lett.* **87**, 132101 (2005).

¹¹W. Shan, W. Walukiewicz, J. W. Ager, E. E. Haller, J. F. Geisz, D. J. Friedman, J. M. Olson, and S. R. Kurtz, *Phys. Rev. Lett.* **82**, 1221 (1999).

¹²J. Wu, W. Shan, and W. Walukiewicz, *Semicond. Sci. Technol.* **17**, 860 (2002).

¹³N. Vogiatzis and J. M. Rorison, *J. Phys.: Condens. Matter* **21**, 255801 (2009).

¹⁴L. Ivanova, H. Eisele, M. P. Vaughan, P. Ebert, A. Lenz, R. Timm, O. Schumann, L. Geelhaar, M. Dähne, S. Fahy, et al., *Phys. Rev. B* **82**, 161210 (2010).

¹⁵J. J. Mudd, N. J. Kybert, W. M. Linhart, L. Buckle, T. Ashley, P. D. C. King, T. S. Jones, M. J. Ashwin, and T. D. Veal, *Appl. Phys. Lett.* **103**, 042110 (2013).

¹⁶A. Lindsay and E. P. O'Reilly, *Phys. Rev. Lett.* **93**, 196402 (2004).

¹⁷M. Seifkar, E. P. O'Reilly, and S. Fahy, *Nanoscale Res. Lett.* **9**, 51 (2014).

¹⁸M. Kondow, K. Uomi, A. Niwa, T. Kitatani, S. Watakiki, and Y. Yazawa, *Jpn. J. Appl. Phys.* **35**, 1273 (1996).

¹⁹M. J. Ashwin, D. Walker, P. A. Thomas, T. S. Jones, and T. D. Veal, *J. Appl. Phys.* **113**, 033502 (2013).

²⁰A. Lindsay, E. P. O'Reilly, A. D. Andreev, and T. Ashley, *Phys. Rev. B* **77**, 165205 (2008).

²¹J. Endicott, A. Patané, J. Ibáñez, L. Eaves, M. Bissiri, M. Hopkinson, R. Airey, and G. Hill, *Phys. Rev. Lett.* **91**, 126802 (2003).

²²V. Virkkala, V. Havu, F. Tuomisto, and M. J. Puska, *Phys. Rev. B* **85**, 085134 (2012).

²³L. Buckle, B. R. Bennett, S. Jollands, T. D. Veal, N. R. Wilson, B. N. Murdin, C. F. McConville, and T. Ashley, *J. Cryst. Growth* **278**, 188 (2005).

²⁴N. Segercrantz and I. Makkonen and J. Slotte and J. Kujala and T. D. Veal and M. J. Ashwin and F. Tuomisto, *J. Appl. Phys.* **118**, 085708 (2015)

²⁵C. Ghezzi, R. Magnanini, A. Parisini, B. Rotelli, L. Tarricone, A. Bosacchi, and S. Franchi, *Phys. Rev. B* **52**, 1463 (1995).

²⁶C. R. Pidgeon and R. N. Brown, *Phys. Rev.* **146**, 575 (1966).

²⁷P. Perlin, P. Wisniewski, C. Skierbiszewski, T. Suski, E. Kaminska, S. G. Subramanya, E. R. Weber, D. E. Mars, and W. Walukiewicz, *Appl. Phys. Lett.* **76**, 1279 (2000).

²⁸K. -F. Berggren and B. E. Sernelius, *Phys. Rev. B* **24**, 1971 (1981).

²⁹M. Muñoz, F. H. Pollak, M. B. Zakia, N. B. Patel, and J. L. Herrera-Pérez, *Phys. Rev. B* **62**, 16600 (2000).

³⁰I. Vurgaftman, J. R. Meyer, L. R. Ram-Mohan, *J. Appl. Phys.* **89**, 5815 (2001).

³¹S. Logothetidis, J. Petalas, M. Cardona, and T. D. Moustakas, *Phys. Rev. B* **50**, 18017 (1994).

³²P. Anderson, *Phys. Rev.* **124**, 41 (1961).